

# The Performance Analysis of RIS-Aided Cooperative NOMA Network for User Relaying without the Direct Link

Hsing-Chung Chen<sup>1,2</sup> Agung Mulyo Widodo<sup>1,3\*</sup> Andika Wisnujati<sup>1,4</sup>  
Prayitno<sup>1,5</sup>

<sup>1</sup> Department of Computer Science and Information Engineering, Asia University, Taiwan

<sup>2</sup> Department of Medical Research, China Medical University Hospital, China Medical University, Taiwan

<sup>3</sup> Department of Computer Science, Esa Unggul University, West Jakarta

<sup>4</sup> Department of Machine Technology, Universitas Muhammadiyah Yogyakarta, Indonesia

<sup>5</sup> Department of Electrical Engineering, Politeknik Negeri Semarang, Indonesia

[cdma2000@asia.edu.tw](mailto:cdma2000@asia.edu.tw), [shin8409@ms6.hinet.net](mailto:shin8409@ms6.hinet.net), [\\*agung.mulyo@esaunggul.ac.id](mailto:*agung.mulyo@esaunggul.ac.id),  
[andikawisnujati@umy.ac.id](mailto:andikawisnujati@umy.ac.id)  
[prayitno@polines.ac.id](mailto:prayitno@polines.ac.id)

## Abstract

In this article, we present a downlink cooperative non-orthogonal multiple access (NOMA) network using Reconfigurable Intelligence Surfaces (RIS)-Aided with the decode-and-forward relay. RIS is fitted with a finite number of elements under Rayleigh's fading channels. The scenario is made by user's relaying without the direct link for near and far users and is addressed in depth. We carefully derive analytical expresses of the probability of loss for several users as the key success metrics. Also, we measure the closed-form expression of coverage likelihood only as a function of statistical channel information. Simulation results are used to verify empirical terms. Diversity of user orders is accomplished in the high signal-to-noise region. Numerical data are provided to verify the feasibility of the proposed RIS-assisted NOMA transmission strategies.

## 1 Introduction

In traditional wireless communication systems, the propagation medium has been considered as an entity that behaves randomly between transmitter and receiver, in which a decrease in the quality of the received signal due to the uncontrolled interaction of transmitted radio waves with surrounding objects is inevitable. The recent presence of reconfigurable smart surfaces (RIS) in wireless communications makes it possible to expand the coverage, by controlling the characteristics of radio waves (scattering,

reflecting, and refraction) to eliminate the negative effects of natural wireless propagation by network operators.

The challenging criteria and possible new usage cases for future 6th generation (6G) and beyond cellular networks that contribute to the future of mobile connectivity look promising. The idea of a reconfigurable smart surfaces is evolving rapidly as a crucial approach to meet the need for huge networking, powered largely by the future Internet of Things (IoT) (Jung, 2019). After the advent of the modern age of wireless communication, the means of transmission has been viewed as a random entity between the transmitter and the receiver, which degrades the efficiency of the obtained signal due to the uncontrollable interference of the transmitting radio waves with the surrounding objects (Basar, 2019). Reconfigurable Intelligence Surface (RIS), which are man-made surface of electromagnetic (EM) material that are electronically controlled with integrated electronics, have received considerable attention due to their unique wireless communication capabilities. The key benefit of RISs is their ability to monitor the transmitting environment and enhance the signal efficiency of the receiver, and thus they can be thought of as allowing environments to be turned into smart ones. Compared to wireless relay technologies, RIS does not require external energy sources and can form wireless signals by soft programming (Yang, 2020). The RIS consists of a huge number of almost passive modules with ultra-low power consumption. Each unit is capable of electronically regulating the phase of the electromagnetic wave event. It achieves this with unnatural properties, including negative refraction, perfect absorption, and anomalous reflection (Dai, 2020) The most advantage of RIS is its artificial planar passive radio array solution, which is highly versatile in terms of cost-effectiveness and energy usage. In specific, by applying an individual phase change to the incident signal, the IRS-adjusted cellular systems reconfigure each passive factor in RIS to vary the channels between the base station (BS) and mobile users constructively or destructively (Hemanth, 2020).

In principle, the electrical size of the unit reflecting elements (i.e., meta-atoms) deployed on RIS is between  $\lambda/8$  and  $\lambda/4$ , where  $\lambda$  is a wavelength of radio frequency (RF) signal (Cui, 2017). Note that conventional large antenna-array systems, such as a massive multiple-input and multiple-output (MIMO) and MIMO relay system, typically require antenna spacing of greater than  $\lambda/2$ . As a result, RIS can provide more efficient and space-intensive communications than traditional antenna array systems, as clearly described in (Jung, 2019). In addition, a large number of reflecting components can be arranged on each RIS, thereby providing precise control of the reflecting wave and enabling it to be coordinated coherently with the desired channel.

The problem in this study is whether the outage probability in RIS-aided wireless has a better performance than the conventional wireless communication model for two users of a signal transmitted by a base station where the analysis carried out in this study is limited to the outages probability without a direct link to rely on. It is to prove whether using RIS-aided wireless can replace conventional relay systems to resolve the attenuation of the signal transmitted by a base station after being received by a receiver. In this case, we use two receivers, such that near the receiver and far receiver. For that purpose, we conduct experiments by making a mathematical model related to the outage probability performance of each receiver, both near and far from the base station, so that the outage probability performance can be compared.

This paper organized as follows. In Section 1, what is RIS and the motivation for this research are introduced. Section 2 presents the related works of this research. In this section 3, our research approach explains how the system model is used and performance analysis through a mathematical approach in order to obtain a mathematical equation plotted in the Cartesian field. Section 4 explains the plot results of the equations obtained and then has a discussion. Finally, we conclude this study in Section 5.

## 2 Related Works

In the previous analysis, examine the asymptotic efficiency of IRS passive beamforming with an exponentially large number of reflective elements and equate it to that of conventional active beamforming/relaying. Simulation results show that the IRS-assisted MIMO system can achieve the same efficiency as the benchmark large MIMO system without the use of IRS, but with greatly reduced active antennas/RF chains. We also draw valuable insights into the optimum implementation of IRS in future wireless networks (Wu, 2019).

Owing to these advantages, the use of an RIS in wireless communication systems has recently received significant attention as in (Tang, 2020). An RIS is typically used for two main wireless communication purposes: a) RIS as an RF chain-free transmitter and b) RIS as a passive beamformer that amplifies the incident waveform (received from a BS) and reflects it to the desired user. In [2], the authors analyzed the error rate performance of a phase-shift keying (PSK) signaling and proved that an RIS transmitter equipped with a large number of reflecting elements can convey information with high reliability. The works in (Tang, W. et al, 2019) and (Tang, W., et al. 2018) proposed RF chain-free transmitter architectures enabled by an RIS that can support PSK and quadrature amplitude modulation (QAM). Meanwhile, the joint active and passive beamformers built in (Q. Wu and R. Zhang, 2018) have been designed to reduce transmission power at BS, under discrete and continuous phase changes, respectively. Also, in (Han, Y., et al, 2018) and (Huang C. et al, 2018), the authors developed a passive beamformer that optimizes ergodic data rate and energy consumption. In addition, the study in (Basar E., et al, 2019) theoretically studied the average symbol error rate (SER) resulting from the ideal passive beamformer and showed that the SER decays exponentially as the number of reflective elements on the RIS increases.

Being a new technology, RIS for applications in wireless communication systems have been recently studied in (Q. Wu, and R. Zhang, 2020); (Bi, S., et al, 2015); (Huang, C. et al. 2019); (Pradhan, C. et al., 2020). For example, the authors of (Q. Wu, and R. Zhang, 2020) proposed using RIS to realize massive device-to-device (D2D) communications where each RIS acts as a signal reflection hub to support simultaneous low-power transmissions through interference mitigation.

It should be remembered that RISs are distinct from other and at first glance, similar systems commonly used in wireless networks, such as relaying, MIMO beam forming, and backscatter communications. Information will be given in the sequence, but it is appropriate to state that the RISs have the following distinguishable features (Basar E., et al. 2019): a) They are nearly passive, and, ideally, they do not need any dedicated energy source, b) They are viewed as a contiguous surface, and, ideally, any point can shape the wave impinging upon it (soft programming), c) They are not affected by receiver noise, since, ideally, they do not need analog-to-digital/digital-to-analog converters (ADCs and DACs), and power amplifiers. As a result, they do not amplify nor introduce noise when reflecting the signals and provide an inherently full-duplex transmission, 4) They have full-band response, since, ideally, they can work at any operating frequency, 5) They can be easily deployed, e.g., on the facades of buildings, ceilings of factories and indoor spaces, human clothing, etc.

In contrast to the above studies, the main contribution of this proposed study is to present an RIS assisted wireless system by comparing the use of RIS assisted wireless in near users and far users which is better than conventional relays which is focused on:

- System without direct link influence from Base Station (BS)
- Consideration of perfect Channel State Information (pCSI) on propagation.
- Obtain the outage probability equation for each condition using a wireless system assisted by RIS as a conventional reflector, relay and relay.
- Knowing the performance of using RIS assisted wireless for users near and far.



### 3 Methods

#### 3.1 System Model

We supposed the system model is depicted in the figure. 1. The transmitted signal,  $s(t)$  from the Base Station (BS) is intended to the two users,  $U_1$  (Near User) and  $U_2$  (Far User).

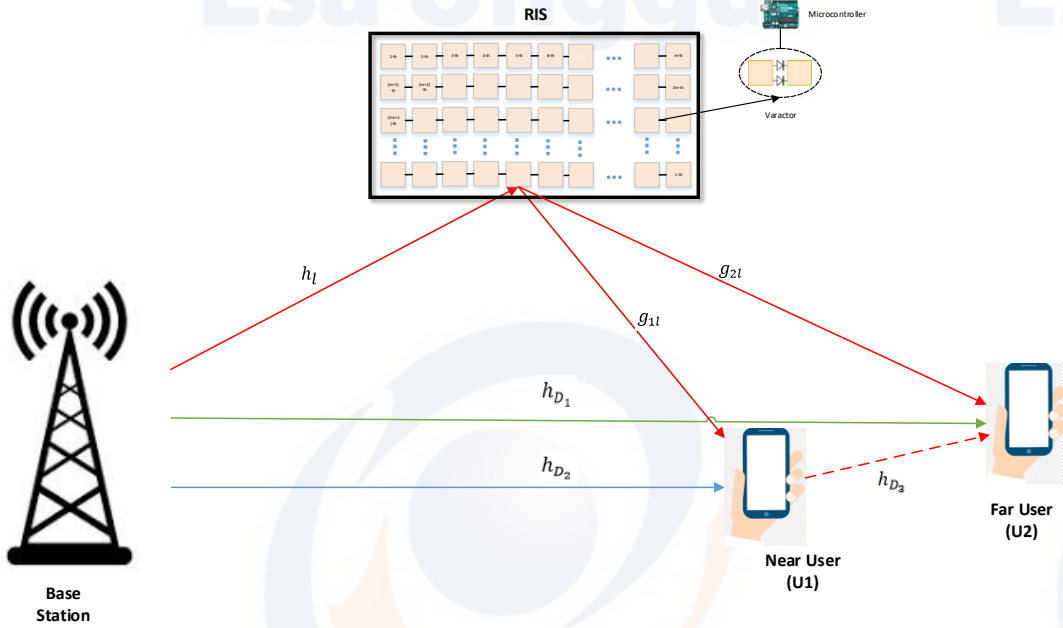


Figure 1. The System Mode

Because the system using NOMA (Non Orthogonal Multiple Acces), the transmitted signal,  $s$  is superimposed of the  $x_1(t)$  and  $x_2(t)$  that are targeted to Near User ( $U_1$ ) and Far User ( $U_2$ ) respectively stand for the data symbol selected modulation (PSK/QAM) constellation. We use the symbols of  $a_1$  and  $a_2$  is the power level of the signal  $x_1(t)$  and  $x_2(t)$  respectively

$$s = \sqrt{\alpha_1 P_s} x_1 + \sqrt{\alpha_2 P_s} x_2 \quad (1)$$

And the received signal by the near user,  $U_1$  from  $S$  is:

$$\begin{aligned} y_{S,U1} &= [h_{D1} + h_{1l}^H \Phi g_{2l}] (\sqrt{\alpha_1 P_s} x_1 + \sqrt{\alpha_2 P_s} x_2) + n_{U1} \quad (2) \\ &= [h_{D1} + \sum_{l=1}^L h_{1l}^H \Phi g_{1l}] (\sqrt{\alpha_1 P_s} x_1 + \sqrt{\alpha_2 P_s} x_2) + n_{U1} \\ &= [\alpha \sum_{l=1}^L h_{1l} g_{1l} e^{j\phi_l} + h_{D1}] (\sqrt{\alpha_1 P_s} x_1 + \sqrt{\alpha_2 P_s} x_2) + n_{U1} \\ &= \left[ (|\hat{h}_{D1}| + e_1) + (\sum_{l=1}^L |\hat{h}_{1l}| |\hat{g}_{1l}| + e'_1) \right] (\sqrt{\alpha_1 P_s} x_1 + \sqrt{\alpha_2 P_s} x_2) + n_{U1} \end{aligned}$$

$$y_{S,U1} = (|\hat{h}_{D1}| + e_1) (\sqrt{\alpha_1 P_s} x_1 + \sqrt{\alpha_2 P_s} x_2) + ((\sum_{l=1}^L |\hat{h}_{1l}| |\hat{g}_{1l}| + e'_1) (\sqrt{\alpha_1 P_s} x_1 + \sqrt{\alpha_2 P_s} x_2)) + n_{U1} \quad (3)$$

Similar above, the received signal by the far user,  $U_2$  from  $S$  is:

$$y_{S,U2} = [|\hat{h}_{D2}| + e_2] (\sqrt{\alpha_1 P_s} x_1 + \sqrt{\alpha_2 P_s} x_2) + (\sum_{l=1}^L |\hat{h}_{1l}| |\hat{g}_{2l}| + e'_2) (\sqrt{\alpha_1 P_s} x_1 + \sqrt{\alpha_2 P_s} x_2) + n_{U2} \quad (4)$$

And the received signal by the far user,  $U_2$  from  $U_1$  :

$$y_{U_1, U_2} = [h_{D_3}] \sqrt{P_r} x_2 + n_{U_2} = [|\hat{h}_{D_3}| + e_3] \sqrt{P_r} x_2 + n_{U_2} \quad (5)$$

Where,  $\alpha_1$  and  $\alpha_2$  is the level power of the signal  $x_1$  and  $x_2$  respectively and  $P_s$  is the signal power of transmitted signal and  $P_r$  is the signal power of the transmission power at  $U_1$ .  $x_1$  and  $x_2$  stand for the data symbol selected modulation (PSK/QAM) constellation.  $n_{U_1}$  and  $n_{U_2}$  are AWGN at  $U_1$  and  $U_2$ , respectively with  $n \sim \mathcal{CN}(0, N_0)$  is the Additive White Gaussian Noise (AWGN) that is modeled as a zero-mean complex Gaussian distribution with variance,  $N_0$ .  $d_{SU_1}$ ,  $d_{SR}$ , and  $d_{RU_1}$  are the distances for  $BS - U_1$ ,  $S - RIS$ , and  $RIS - U_1$ .  $\chi$  is the path loss exponent, then  $h_{D_1}$ ,  $h_l$  and  $g_{1l}$  is fading coefficient that is represented by a Complex Gaussian Random Variables (RV) with zero mean and unit variance.  $\phi_l$  is the adjustable phase applied by the  $l$ -th reflecting element of RIS.  $\eta$  is the relative channel estimation error.  $\beta$  is the expected value, and the  $\alpha \in (0, 1]$  is the amplitude reflection coefficient with  $\alpha = 1$  corresponding to lossless reflection.

### 3.2 Performance Analysis

According to figure 1, we divide the model become two parts, i.e Near User ( $U_1$ ) and Far User ( $U_2$ ). At the Near user,  $U_1$ . Based on the assumption of power allocation coefficients, the signal of  $U_2$  is decoded firstly by exploiting successive interference cancellation from the received superposed signal at  $U_1$ , where  $U_2$  with more transmit power has less the inter-user interference. The received signal to interference and noise ratio (SINR) for  $U_1$  to decode signal  $x_2$  of  $U_2$  can be expressed as

$$\rho_{U_1 \rightarrow U_2} = \frac{|\sum_{l=1}^L \hat{h}_l \hat{g}_{1l}|^2 \alpha_2 \rho_s + |\hat{h}_{D_1}|^2 \alpha_2 \rho_s}{(|h_{D_1}|^2 + |\sum_{l=1}^L \hat{h}_l \hat{g}_{1l}|^2) \alpha_1 \rho_s + \eta_1 (d_{SU_1})^{-\chi} \rho_s + \eta_2 L (d_{SR})^{-\chi} (d_{RU_1})^{-\chi} \rho_s + 1} \quad (6)$$

$$\rho_{U_1 \rightarrow U_2} = \frac{(|\sum_{l=1}^L \hat{h}_l \hat{g}_{1l}|^2 + |\hat{h}_{D_1}|^2) \alpha_2 \rho_s}{(|h_{D_1}|^2 + |\sum_{l=1}^L \hat{h}_l \hat{g}_{1l}|^2) \alpha_1 \rho_s + \eta_1 (d_{SU_1})^{-\chi} \rho_s + \eta_2 L (d_{SR})^{-\chi} (d_{RU_1})^{-\chi} \rho_s + 1}$$

Where,  $\rho_s = \frac{P_s}{N_0}$ , is the transmit signal to noise ratio (SNR).

$$\rho_{U_1, x_1} = \frac{(|\sum_{l=1}^L \hat{h}_l \hat{g}_{1l}|^2 + |\hat{h}_{D_1}|^2) \alpha_1 \rho_s}{\eta_1 (d_{SU_1})^{-\chi} \rho_s + \eta_2 L (d_{SR})^{-\chi} (d_{RU_1})^{-\chi} \rho_s + 1} \quad (7)$$

and we define,  $\hat{X}_1 + e_1' = |\sum_{l=1}^L \hat{h}_l^H \Phi \hat{g}_{1l}|^2 + |\hat{h}_{D_1}|^2 + e_1'$ , then its mean is obtained by the independence of channels as :

$$\mathbb{E}\{\hat{X}\} = \mathbb{E}\{|\hat{h}_D|^2\} + \mathbb{E}\{|\sum_{l=1}^L \hat{h}_l^H \Phi \hat{g}_{1l}|^2\} = \beta_{SU} + L \beta_{SR} \beta_{RU}$$

Which is obtained due to circular symmetric properties.

$$\mathbb{E}\{|\hat{X}|^2\} = \mathbb{E}\{(|\hat{h}_D|^2 + |\sum_{l=1}^L \hat{h}_l^H \Phi \hat{g}_{1l}|^2)^2\}$$

$$\mathbb{E}\{|\hat{X}|^2\} = \mathbb{E}\{(|\hat{h}_D|^2 + \hat{h}_D^* \hat{h}_l^H \Phi \hat{g}_{1l} + \hat{h}_D \hat{g}_{1l}^H \Phi^H \hat{h}_l + |\hat{h}_l^H \Phi \hat{g}_{1l}|^2)^2\}$$

$$\mathbb{E}\{|\hat{X}|^2\} = \mathbb{E}\{a + b + c + d\}^2$$

$$\mathbb{E}\{|\hat{X}|^2\} = \mathbb{E}\{a^2\} + \mathbb{E}\{b^2\} + \mathbb{E}\{c^2\} + 2\mathbb{E}\{ad\} + \mathbb{E}\{d^2\}$$

Where;

$$\mathbb{E}\{a^2\} = 2\beta_{SU}^2; \mathbb{E}\{b^2\} = \mathbb{E}\{c^2\} = L\beta_{SU}\beta_{SR}\beta_{RU}; \mathbb{E}\{ad\} = L\beta_{SU}\beta_{SR}\beta_{RU}; \text{ and}$$

$$\mathbb{E}\{d^2\} = (2L^2 + 2L)\beta_{RU}^2\beta_{SU}^2$$

$$\mathbb{E}\{|\hat{X}_1|^2\} = 2\beta_{SU}^2 + 4L\beta_{SU}\beta_{SR}\beta_{RU} + (2L^2 + 2L)\beta_{RU}^2\beta_{SU}^2$$

$$\text{Var}\{\hat{X}_1\} = \mathbb{E}\{|\hat{X}_1|^2\} - |\mathbb{E}\{\hat{X}_1\}|^2 = \beta_{SU}^2 + 2L\beta_{SU}\beta_{SR}\beta_{RU} + (L^2 + 2L)\beta_{RU}^2\beta_{SU}^2$$

$$m = \frac{(\mathbb{E}\{\hat{X}\})^2}{\text{Var}\{\hat{X}\}} = \frac{(\beta_{SU} + L\beta_{SR}\beta_{RU})^2}{\beta_{SU}^2 + 2L\beta_{SU}\beta_{SR}\beta_{RU} + (L^2 + 2L)\beta_{RU}^2\beta_{SU}^2} = \frac{(\beta_{SU} + L\beta_{SR}\beta_{RU})^2}{(\beta_{SU} + L\beta_{SR}\beta_{RU})^2 + 2L\beta_{RU}^2\beta_{SU}^2}$$

$$\vartheta = \frac{\text{Var}\{\hat{X}\}}{\mathbb{E}\{\hat{X}\}} = \frac{(\beta_{SU} + L\beta_{SR}\beta_{RU})^2 + 2L\beta_{SR}^2\beta_{RU}^2}{\beta_{SU} + L\beta_{SR}\beta_{RU}} = \beta_{SU} + L\beta_{SR}\beta_{RU} + \frac{2\beta_{SR}^2\beta_{RU}^2}{\beta_{SU} + L\beta_{SR}\beta_{RU}}$$

Similar above, if:

$$\begin{aligned} \hat{X}_1 + e'_1 &= \left| \sum_{l=1}^L \hat{h}_{1l}^H \Phi \hat{g}_{1l} \right|^2 + |\hat{h}_{D_1}|^2 + e'_1 \\ \mathbb{E}\left\{ \left| \hat{X}_1 + e'_1 \right|^2 \right\} &= \left( \beta_{SU_1} + \eta_1 (d_{SU_1})^{-\kappa} \right) + L(\beta_{SR} + \eta_2 (d_{SR})^{-\kappa}) (\beta_{RU_1} + \eta_3 (d_{RU_1})^{-\kappa}) \\ m_1 &= \frac{(\mathbb{E}\{\hat{X}_1 + e'_1\})^2}{\text{Var}(\hat{X}_1 + e'_1)} \\ &= \frac{\left( (\beta_{SU_1} + \eta_1 (d_{SU_1})^{-\kappa}) + L(\beta_{SR} + \eta_2 (d_{SR})^{-\kappa}) (\beta_{RU_1} + \eta_3 (d_{RU_1})^{-\kappa}) \right)^2}{\left( (\beta_{SU_1} + \eta_1 (d_{SU_1})^{-\kappa}) + L(\beta_{SR} + \eta_2 (d_{SR})^{-\kappa}) (\beta_{RU_1} + \eta_3 (d_{RU_1})^{-\kappa}) \right)^2 + 2L(\beta_{SR} + \eta_2 (d_{SR})^{-\kappa})^2 (\beta_{RU_1} + \eta_3 (d_{RU_1})^{-\kappa})^2} \\ \vartheta_1 &= \frac{\text{Var}(\hat{X}_1 + e'_1)}{\mathbb{E}\{\hat{X}_1 + e'_1\}} = \left( \beta_{SU_1} + \eta_1 (d_{SU_1})^{-\kappa} \right) + L(\beta_{SR} + \eta_2 (d_{SR})^{-\kappa}) (\beta_{RU_1} + \eta_3 (d_{RU_1})^{-\kappa}) + \\ &\frac{2L(\beta_{SR} + \eta_2 (d_{SR})^{-\kappa})^2 (\beta_{RU_1} + \eta_3 (d_{RU_1})^{-\kappa})^2}{\left( (\beta_{SU_1} + \eta_1 (d_{SU_1})^{-\kappa}) + L(\beta_{SR} + \eta_2 (d_{SR})^{-\kappa}) (\beta_{RU_1} + \eta_3 (d_{RU_1})^{-\kappa}) \right)} \end{aligned}$$

Now, we consider the network coverage probability, defined for either an arbitrary or optimal phase shift as follows.

By setting,  $\rho_{Th_1} = \frac{(2^{R_1-1})}{\rho_s}$  and  $\rho_{Th_2} = \frac{(2^{R_2-1})}{\rho_s}$  then  $\tau_1 = \frac{\lambda_1 \rho_{Th_1}}{(\alpha_1 \rho_s)}$ ,  $\tau_2 = \frac{\lambda_1 \rho_{Th_2}}{(\alpha_2 - \alpha_1 \rho_{Th_2}) \rho_s}$ , and  $\lambda_1 =$

$\eta_1 (d_{SU_1}^{-\kappa}) \rho_s + L \eta_2 (d_{SR}^{-\kappa}) \rho_s \cdot \eta_3 (d_{RU_1}^{-\kappa}) \rho_s + 1$ ,  $\delta_1 = \frac{1}{\vartheta_1}$ , where,  $\alpha_2 > \alpha_1 \rho_{Th_2}$ , then

$\Gamma(m_1) = \int_0^\infty y^{m_1-1} e^{-y} dy$  and  $\gamma(m_1, y) = \int_0^y y^{m_1-1} e^{-y} dy$ ;  $\Gamma(m_1) = (m_1 - 1)!$

And,  $\gamma(m_1, y) = (m_1 - 1)! \left[ 1 - e^{-y} \sum_{l=0}^{m_1-1} \left( \frac{y^l}{l!} \right) \right]$

$$\Gamma(m_1) = (m_1 - 1)!, \text{ and } \gamma\left(m_1, \frac{z}{\vartheta_1}\right) = (m_1 - 1)! \left[ 1 - e^{-\frac{z}{\vartheta_1}} \sum_{l=0}^{m_1-1} \frac{\left(\frac{z}{\vartheta_1}\right)^l}{l!} \right]$$

$$\text{Thus, } P_{U_1} = \frac{\gamma\left(m_1, \frac{z}{\vartheta_1}\right)}{\Gamma(m_1)} = \frac{(m_1-1)! \left[ 1 - e^{-\frac{z}{\vartheta_1}} \sum_{l=0}^{m_1-1} \frac{\left(\frac{z}{\vartheta_1}\right)^l}{l!} \right]}{(m_1-1)!} = 1 - e^{-\frac{z}{\vartheta_1}} \sum_{l=0}^{m_1-1} \frac{\left(\frac{z}{\vartheta_1}\right)^l}{l!}$$

In this case:

$$P_{U_1} = 1 - Pr(X > \tau_2, X > \tau_1)$$

$$P_{U_1} = 1 - Pr(X > \max(\tau_2, \tau_1))$$

$$P_{U_1} = 1 - \left( e^{-\frac{z}{\vartheta_1}} \sum_{j=0}^{m_1-1} \frac{\left(\frac{z}{\vartheta_1}\right)^j}{j!} \right)$$

$$P_{U_1} = 1 - e^{-\delta_1 \tau} \sum_{j=0}^{m_1-1} \frac{(\delta_1 \tau)^j}{j!} \quad (8)$$

At the far user, U2 only needs to treat signal  $x_1$  of U1 as noise to decode its own signal. The received SINR for U2 to decode its own signal  $x_2$  is given by

$$\rho_{1,U_2} = \frac{|h_{D_2}|^2 + \left| \sum_{l=1}^L |h_l| |g_{2l}| \right|^2 \alpha_2 \rho_s}{\left| |h_{D_2}|^2 + \left| \sum_{l=1}^L |h_l| |g_{2l}| \right|^2 \right| \alpha_1 \rho_s + \eta_2 (d_\mu)^{-\kappa} \rho_s + 1} \quad (9)$$

The received SINR for U2 to decode signal  $x_2$  for relaying link is given by

$$\rho_{2,U_2} = \frac{|h_{D_3}|^2 \rho}{\eta_3 (d_\mu)^{-\kappa} \rho + 1}$$

The received SINR after selection combining (SC) at U2 is given by

$$\rho_{U_2}^{SC} = \frac{\|h_{D_3}\|^2 \rho}{\eta_3 (d_\mu)^{-\kappa} \rho + 1} + \frac{\|h_{D_2}\| + \sum_{l=1}^L |h_{l1}| |g_{2l}|^2 \alpha_2 \rho_s}{\|h_{D_2}\| + \sum_{l=1}^L |h_{l1}| |g_{2l}|^2 \alpha_1 \rho_s + \eta_2 (d_\mu)^{-\kappa} \rho_s + 1} \quad (10)$$

In the first scenario, **the outage events of U2 occur if one of the following two events is satisfied.**

**The first event** is that U1 fails to decode the signal  $x_2$ . The second event is that U2 fails to decode its own signal  $x_2$  when U1 can successfully decode the signal  $x_2$ . Based on the above events, the outage probability of U2 can be expressed as follows:

$$P_{U_2, NoDir} = P_r(\rho_{1,U_2} < \rho_{Th_2}) + P_r(\rho_{2,U_2} < \rho_{Th_2}, \rho_{1,U_2} > \rho_{Th_2})$$

If,  $\hat{X}_2 = |\hat{h}_{2l}^H \Phi \hat{g}_{2l}|^2 + |\hat{h}_{D_2}|^2$ , then its mean is obtained by the independence of channels as :

$$\mathbb{E}\{\hat{X}_2\} = \mathbb{E}\{|\hat{h}_{D_2}|^2\} + \mathbb{E}\{|\hat{h}_{2l}^H \Phi \hat{g}_{2l}|^2\} = \beta_{SU_2} + L\beta_{SR}\beta_{RU_2}$$

The using the similar steps above, it can be obtained Which is obtained due to circular symmetric properties.

$$\mathbb{E}\{|\hat{X}_2|^2\} = 2\beta_{SU_2}^2 + 4L\beta_{SU_2}\beta_{SR}\beta_{RU_2} + (2L^2 + 2L)\beta_{RU_2}^2\beta_{SR}^2$$

$$Var\{\hat{X}_2\} = \mathbb{E}\{|\hat{X}_2|^2\} - |\mathbb{E}\{\hat{X}_2\}|^2 = \beta_{SU_2}^2 + 2L\beta_{SU_2}\beta_{SR}\beta_{RU_2} + (L^2 + 2L)\beta_{SR}^2\beta_{RU_2}^2$$

$$\hat{X}_2 + e'_2 = |\sum_{l=1}^L \hat{h}_{2l}^H \Phi \hat{g}_{2l}|^2 + |\hat{h}_{D_2}|^2 + e'_2$$

$$\mathbb{E}\{|\hat{X}_2 + e'_2|^2\} = (\beta_{SU_2} + \eta_4 (d_{SU_2})^{-\kappa}) + L(\beta_{SR} + \eta_5 (d_{SR})^{-\kappa})(\beta_{RU_2} + \eta_6 (d_{RU_2})^{-\kappa})$$

So that, it can be obtained the equation as follows.

$$m_2 = \frac{((\beta_{SU_2} + \eta_4 (d_{SU_2})^{-\kappa}) + L(\beta_{SR} + \eta_5 (d_{SR})^{-\kappa})(\beta_{RU_2} + \eta_6 (d_{RU_2})^{-\kappa}))^2}{((\beta_{SU_2} + \eta_4 (d_{SU_2})^{-\kappa}) + L(\beta_{SR} + \eta_5 (d_{SR})^{-\kappa})(\beta_{RU_2} + \eta_6 (d_{RU_2})^{-\kappa}))^2 + 2L(\beta_{SR} + \eta_5 (d_{SR})^{-\kappa})(\beta_{RU_2} + \eta_6 (d_{RU_2})^{-\kappa})^2}$$

$$\vartheta_2 = (\beta_{SU_2} + \eta_4 (d_{SU_2})^{-\kappa}) + L(\beta_{SR} + \eta_5 (d_{SR})^{-\kappa})(\beta_{RU_2} + \eta_6 (d_{RU_2})^{-\kappa}) + \frac{2L(\beta_{SR} + \eta_5 (d_{SR})^{-\kappa})(\beta_{RU_2} + \eta_6 (d_{RU_2})^{-\kappa})^2}{(\beta_{SU_2} + \eta_4 (d_{SU_2})^{-\kappa}) + L(\beta_{SR} + \eta_5 (d_{SR})^{-\kappa})(\beta_{RU_2} + \eta_6 (d_{RU_2})^{-\kappa})}$$

Then,  $\hat{Y} = |\hat{h}_{D_3}|^2$ , then its mean is obtained by the independence of channels as :

$$\mathbb{E}\{\hat{Y}\} = \mathbb{E}\{|\hat{h}_{D_3}|^2\} = \beta_{U_1U_2}$$

Which is obtained due to circular symmetric properties.

$$\mathbb{E}\{|\hat{Y}|^2\} = \mathbb{E}\{|\hat{h}_{D_3}|^4\}$$

$$\text{For, } \mathbb{E}\{|\hat{Y}|^2\} = \mathbb{E}\{|a|^2\} \text{ and}$$

$$\mathbb{E}\{|\hat{Y}|^2\} = \mathbb{E}\{|a|^2\} = 2\beta_{U_1U_2}^2 \text{ and } Var\{\hat{Y}\} = \mathbb{E}\{|\hat{Y}|^2\} - |\mathbb{E}\{\hat{Y}\}|^2 = 2\beta_{U_1U_2}^2 - \beta_{U_1U_2}^2 = \beta_{U_1U_2}^2,$$

then

$$\mathbb{E}\{\hat{Y} + e_3\} = (\beta_{U_1U_2} + \eta_7 (d_{U_1U_2})^{-\kappa})$$

$$\mathbb{E}\{|\hat{Y} + e_3|^2\} = 2(\beta_{U_1U_2} + \eta_7 (d_{U_1U_2})^{-\kappa})^2$$

So that,

$$m_3 = \frac{(\mathbb{E}\{\hat{Y}\})^2}{Var\{\hat{Y}\}} = \frac{\beta_{U_1U_2}^2}{\beta_{U_1U_2}^2} = 1$$

$$\vartheta_3 = \frac{Var\{\hat{Y}\}}{\mathbb{E}\{\hat{Y}\}} = \frac{\beta_{U_1U_2}^2}{\beta_{U_1U_2}} = \beta_{U_1U_2}$$

$$Var\{\hat{Y} + e_3\} = \mathbb{E}\{|\hat{Y} + e_3|^2\} - |\mathbb{E}\{\hat{Y} + e_3\}|^2 = (\beta_{U_1U_2} + \eta_7 (d_{U_1U_2})^{-\kappa})^2 = \beta_{U_1U_2}^2 + 2\beta_{U_1U_2}\eta_7 (d_{U_1U_2})^{-\kappa} + (\eta_7 (d_{U_1U_2})^{-\kappa})^2$$

Similar to above, for arbitrary phase shifts, the coverage probability is computed as



$$P_{U_2, NoDir} = 1 - e^{-(\delta_2 \tau_2 + \delta_3 \tau_3)} \sum_{j=0}^{m_1-1} \sum_{k=0}^{m_2-1} \frac{(\delta_1 \tau_2)^j (\delta_2 \tau_3)^k}{j! k!} \quad (11)$$

Where,  $\tau_3 = \frac{\lambda_2 \rho_s \tau h_2}{\rho_s}$ ,  $\lambda_2 = \eta_2 d_{\mu}^{-\kappa} \rho_s + 1$ , and  $\delta_2 = \frac{1}{\vartheta_2}$ ,  $\delta_3 = \frac{1}{\vartheta_3}$

## 4 Result and Discussion

Numerical results are presented in this section to evaluate the outage performance of the cooperative NOMA network with pCSI in terms of possible outages via the Rayleigh fading channel. MATLAB programming software is used for making simulations by setting reasonable parameters. All of the above analyzes were numerically verified using an arrangement where the locations were mapped into the Cartesian coordinate system. Specifically, the source (S) is located at (0, 0) and the IRS at (40, 10). Assuming the positions of BS,  $U_1$ , and  $U_2$  are in a straight line. We generalize that the distance between BS and  $U_2$  is normalized to one, that is,  $d_0 = 1$ , and we can obtain  $d_2 = 1 - d_1$ , where  $d_1$  and  $d_2$  are the normalized distances between BS and  $U_1$ , and between  $U_1$  and  $U_2$ . The following table 1 sets the simulation parameters.

**Table 1. Simulation Parameters**

Description	NOMA
Power allocation coefficient	$\alpha_1 = 0.2, \alpha_2 = 0.8$
Path loss exponent	$\kappa = 2$
Fading parameter	$m_1 = m_2 = 1$
Relative channel estimation error	$\eta_1 = \eta_2 = 1 \times 10^{-4} \sim 9 \times 10^{-4}$
Distance between two nodes	$d_{SU_1} = 0.04 (40 \text{ m}), d_{SU_2} = 0.04 \sim 1, d_{SR} = 0.04 (40 \text{ m}),$ $d_{U_1 U_2} = 1 - d_{SU_1}, d_{RU_1} = 1, d_{RU_2} = 0.04 \sim 1$
Transmit SNR	$\rho_s = 0 \sim 50 \text{ dB}$
The antenna gain at transmitter and receiver	$G_t = 3, 2 \text{ dBi}, G_r = 1.3 \text{ dBi}$
Target Rate	$R_1 = 3, 6 \text{ BPCU}, R_2 = 1 \text{ BPCU}$

Then using the eq. (8), we can be obtained the plotting Outage Probability versus transmit signal–noise–ratio (SNR) as follows.

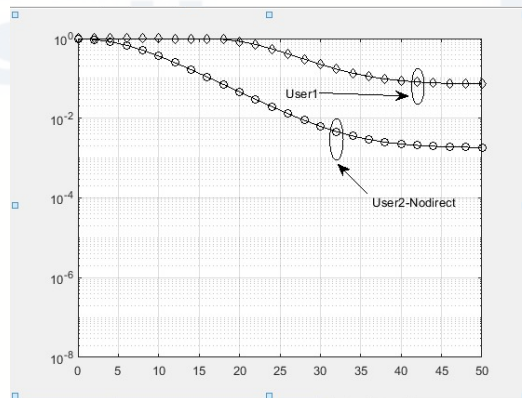


Figure 2: The Outage Probability versus transmit signal–noise–ratio (SNR)



The approximate user pair outage probability curves are plotted according to (6), (7), (8), and (9) respectively. It is observed that the outage probability decreases as the transmission SNR increases at low SNR and reaches a fixed value at high SNR. The fault floor exists at a high SNR due to channel estimation errors, leading to zero order diversity. We suspect, since  $U_2$  only receives signals from the link relay while  $U_2$  receives signals from the link relay and direct link in the next scenario, the reliability of the signal received by  $U_2$  in the second scenario has been improved.

Furthermore, we model the large-scale-fading coefficient [dB] at near user by  $\beta_\mu = G_t + G_r + 10\chi_\mu \log_{10} \left( \frac{d_\mu}{1m} \right) - 30 + z_\mu$  where  $\mu \in \{SU_1, SR, RU_1\}$  and  $z_\mu =$  shadow fading.

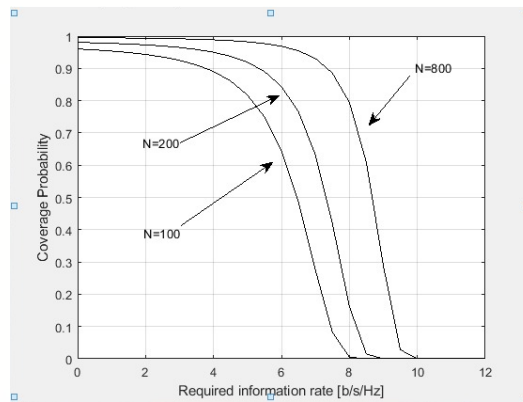


Figure 3: The graphics of Outage Probability versus the required information rate at Near User

Figure. 2 plots the coverage (outage probability) versus the level of different required information, where the destination is located (40, 0), while the shadow fading  $z_\mu = 0$  and a number the phase shift is  $N = 100, 200, 800$ .

From this figure, it can be seen that the greater the number of RIS elements, then the greater the probability coverage is obtained for scenarios without a direct relay. Likewise for the amount of the required information rate it also gets bigger as the number of  $N$ .

## 5 Conclusion

This paper has used the incomplete Gamma distribution and Rayleigh channel statistical information to obtain closed-form expressions of possible coverage for optimal or arbitrary IRS enhanced communications. In contrast to previous studies, in this study, we consider the Rayleigh channel error.

Performance analysis is carried out for near and far users. From the simulation results we have done, it can be seen that usage of RIS-Aided in the NOMA communication system can actually increase the probability of coverage and the number of information rates required is proportional to the greater the number of RIS elements.

## References

M. Jung, W. Saad, M. Debbah, and C. S. Hong, "On the optimality of reconfigurable intelligent surfaces (RISs): Passive beamforming, modulation, and resource allocation," *arXiv preprint arXiv:1910.00968*, 2019.

E. Basar, M. Di Renzo, J. De Rosny, M. Debbah, M.-S. Alouini, and R. Zhang, "Wireless communications through reconfigurable intelligent surfaces," *IEEE Access*, vol. 7, pp. 116753-116773, 2019.

L. Yang, F. Meng, Q. Wu, D. B. da Costa, and M.-S. Alouini, "Accurate closed-form approximations to channel distributions of RIS-aided wireless systems," *IEEE Wireless Communications Letters*, vol. 9, no. 11, pp. 1985-1989, 2020.

L. Dai *et al.*, "Reconfigurable intelligent surface-based wireless communications: Antenna design, prototyping, and experimental results," *IEEE Access*, vol. 8, pp. 45913-45923, 2020.

A. Hemanth, K. Umamaheswari, A. C. Pogaku, D.-T. Do, and B. M. Lee, "Outage Performance Analysis of Reconfigurable Intelligent Surfaces-Aided NOMA under Presence of Hardware Impairment," *IEEE Access*, 2020.

Y. Cui, T. Jiang, S. Yu, R. Wu, and W. Gu, "Passive-compensation-based stable rf phase dissemination for multiaccess trunk fiber link with anti-gvd and anti-backscattering function," *IEEE Photonics Journal*, vol. 9, no. 5, pp. 1-8, 2017.

Q. Wu and R. Zhang, "Intelligent reflecting surface enhanced wireless network via joint active and passive beamforming," *IEEE Transactions on Wireless Communications*, vol. 18, no. 11, pp. 5394-5409, 2019.

W. Tang *et al.*, "Wireless communications with reconfigurable intelligent surface: Path loss modeling and experimental measurement," *IEEE Transactions on Wireless Communications*, 2020.

Trinh Van Chien, Lam Thanh Tu, Symeon Chatzinota, and Bjorn Ottersten., "Coverage Probability and Ergodic Capacity of Intelligent Reflecting Surface-Enhanced Communication Systems," *IEEE Communications Letters*, 2020.

Xianli Gong, Xinwei Yue, and Feng Liu., " Performance Analysis of Cooperative NOMA Networks with Imperfect CSI over Nakagami-m Fading Channels," *Sensors* 2020, 20, 424.